

Atomic imaging in EBCO superconductor films by an X-ray holography system using a toroidally bent graphite analyzer

Tsuguhisa Sekioka,^{a*} Kouichi Hayashi,^b Eiichiro Matsubara,^b Yukio Takahashi,^c Tetsutaro Hayashi,^c Mititaka Terasawa,^d Tohru Mitamura,^a Akihiro Iwase^e and Osamu Michikami^f

^aGraduate School of Engineering, University of Hyogo, 2167 Shosha, Himeji, Hyogo 671-2201, Japan, ^bInstitute for Materials Research, Tohoku University, 2-1-1 Katahira, Aoba-ku, Sendai, Miyagi 980-8577, Japan, ^cDepartment of Materials Science, Graduate School of Engineering, Tohoku University, Katahira, Aoba-ku, Sendai, Miyagi 980-8577, Japan, ^dLaboratory of Advanced Science and Technology for Industry (LASTI), University of Hyogo, 3-1-2 Kouto, Kamigori-cho, Ako-gun, Hyogo 678-1205, Japan, ^eResearch Institute for Advanced Science and Technology, Osaka Prefecture University, 1-1 Gakuen-cho, Sakai, Osaka 599-8531, Japan, and ^fFaculty of Engineering, Iwate University, 3-18-8 Ueda, Morioka, Iwate 020-8550, Japan.
E-mail: sekioka@eng.u-hyogo.ac.jp

X-ray fluorescence holography (XFH) is a new technique enabling the determination of the three-dimensional local atomic structure around a certain element. This method has been applied to analyze the local structure around Cu in 300 nm thin films of $\text{EuBa}_2\text{Cu}_3\text{O}_{7-\delta}$ (EBCO) epitaxially grown on MgO (100) substrate, using the newest system for XFH measurement and high-brilliance synchrotron radiation at SPring-8. Here, the results of a study on the irradiation effect on the local atomic structure of EBCO superconductor with XFH measurements are presented.

1. Introduction

X-ray fluorescence holography (XFH) is a promising tool for determining the local structure around a specified atom. Szöke (1986) suggested that interference patterns generated by radiation from atomic sources inside a solid, *e.g.* photoelectrons or fluorescent X-rays, can be thought of as a holographic record and that meaningful real-space images can be reconstructed from them. This was proved in an X-ray photoelectron holography experiment in 1990 (Harp *et al.*, 1990). Six years later, Tegze & Faigel (1996) succeeded in imaging the atomic arrangement in a SrTiO_3 single crystal by measuring the X-ray fluorescence hologram. In order to extract an extremely weak holographic signal of 10^{-3} , a few months were required for the measurement. Subsequently, its time-reversed version was demonstrated by Gog *et al.* (1996) using hematite (Fe_2O_3). This method, which is called multiple-energy holography or inverse XFH, can record several holograms at different X-ray energies, and thus can produce a fine atomic image without artifacts and twin images. Up to now, XFH has been applied to various materials, such as Zn dopants in GaAs (Hayashi, Mitsui *et al.*, 2001), AlPdMn quasi crystals (Marchesini *et al.*, 2000), FePt magnetic thin films (Takahashi *et al.*, 2003) and SiGe (Hayashi *et al.*, 2004).

We have applied the XFH technique to analyze the local structure around Cu in $\text{EuBa}_2\text{Cu}_3\text{O}_{7-\delta}$ (EBCO) superconductor irradiated by high-energy heavy ions. In oxide superconductors, it is well known that a highly damaged region is produced along the path of heavy ions of energy of several hundred MeV or GeV. Such 'columnar defects' can effectively pin the quantized magnetic flux and are quite useful for the enhancement of superconducting critical current density. High- T_c superconductors irradiated by high-energy heavy ions show a remarkable electrical resistivity increase, magnetization and superconductivity enhancement. The effects of these defects on the material properties have been extensively studied (Blatter *et al.*, 1994; Iwase *et al.*, 1998). However, the correlation between the crystal structure change and the superconductivity is not clearly understood. We report here an evaluation of the local atomic structure of virgin and irradiated EBCO samples for understanding this correlation between crystal structure and superconductivity.

One of the authors constructed the XFH apparatus at the SPring-8 synchrotron radiation facility (Hayashi, Miyake *et al.*, 2001). We recently installed a toroidally bent graphite analyzer and measured the holograms of virgin and irradiated EBCO thin films. From the reconstructed atomic images of

both samples, the structural change caused by heavy-ion irradiation was determined and is discussed here.

2. Experimental procedure

The specimens were EBCO thin films epitaxially grown on MgO (100) substrate by means of RF magnetron sputtering (Michikami *et al.*, 1990). The films were *c*-axis oriented and the thickness was about 300 nm, and 5 mm × 5 mm in size. The superconducting transition temperature, T_c , was 80–89 K. XFH measurements were performed for the EBCO specimen irradiated parallel to the *c*-axis at room temperature with 210 MeV I ions from a tandem accelerator at the Japan Atomic Energy Research Institute, at a fluence of $5 \times 10^{11} \text{ cm}^{-2}$; similar measurements were also performed for an unirradiated specimen. Since the projected range for the irradiation was much larger than the specimen thickness, the energy loss of ions in the specimen was much smaller than the initial ion energy, and the irradiating ions did not remain in the specimen as impurities. θ - 2θ X-ray diffraction (XRD) measurements were carried out for the unirradiated and irradiated EBCO specimens in 0.05° steps in θ , in order to investigate the irradiation damage effect on the *c*-axis lattice parameter. As a result, the relative increase in the *c*-axis lattice parameter of the irradiated specimen compared well with that of the unirradiated specimen, $\Delta c/c_0$, is 0.6%. The relative error of this value was estimated at 20%, determined by the full width at half-maximum of the XRD peak. This value is consistent with previously published data on the relative increase in the *c*-axis parameter as a function of ion-fluence for EBCO film irradiated with high-energy heavy ions (Iwase *et al.*, 1998). Furthermore, since an obvious difference in the peak width for both samples was not recognized, this implies that the stacking structure was not largely destroyed by irradiation.

Here, we intended to use XFH to image the atomic structure around Cu in the EBCO superconductor. The holographic measurements were performed at synchrotron radiation beamline BL37XU at SPring-8. The electron storage-ring current was between 100 and 80 mA during measurements. The synchrotron radiation from an in-vacuum undulator was monochromated by a Si(111) double-crystal monochromator. Fig. 1 shows the experimental set-up. K_α X-ray fluorescence from Cu was detected using a combination system of an avalanche photodiode (APD) and toroidally bent graphite as a fluorescence detector. The APD has an energy resolution of $\sim 10\%$ and can collect X-rays at high count rates of $\sim 10^8 \text{ counts s}^{-1}$. The fluorescence Cu K_α characteristic X-rays were analyzed and focused in front of the detector by the toroidally bent graphite crystal with a 30 mm radius and mosaic spread of $\sim 1^\circ$ (Matsushita Electric). This analyzer was designed for focusing the Cu K_α characteristic X-rays. The focusing efficiency of this analyzer was measured using the Cu K_α characteristic X-rays from a rotating-anode X-ray generator with a copper target. Using this analyzer, the intensity of the Cu K_α characteristic X-rays through a pinhole of diameter 2 mm at the focal point of the analyzer was 240-

fold, as large as that without using this analyzer. The solid angle collected by the analyzer was 0.235 sr. The signal from the APD was processed by a signal divider, two discriminators and a scaler in order to extract the pure Cu K_α X-ray signal from the APD output signal.

XFH measurements were performed at photon energies of 18.0, 18.25, 18.5, 18.75 and 19.0 keV for both unirradiated and irradiated EBCO specimens. The yield of Cu K_α X-ray fluorescence was measured as a function of the azimuthal angle φ and polar angle θ within the ranges $0^\circ \leq \varphi \leq 360^\circ$ and $0^\circ \leq \theta \leq 70^\circ$. Since the fluorescence analyzing system rotates together with the polar angle θ , the exit angle of the X-ray fluorescence was fixed at 45° . The dwelling time for one pixel was 0.1 s with 0.3° steps in φ and 1° steps in θ . The highest count rate was more than $2 \times 10^6 \text{ counts s}^{-1}$. The hologram at each energy could be measured in 2.5 h.

3. Results and discussion

Figs. 2(a) and 2(b) show holograms of EBCO unirradiated (a) and irradiated with 210 MeV I ions at a fluence of $5 \times 10^{11} \text{ cm}^{-2}$ (b), respectively, measured at a photon energy of 18.0 keV. The sharp X-ray standing-wave (XSW) lines resulting from the long-range periodic structure of EBCO appear in both holograms, indicating the fourfold and mirror symmetries. In order to improve the statistical accuracy, the

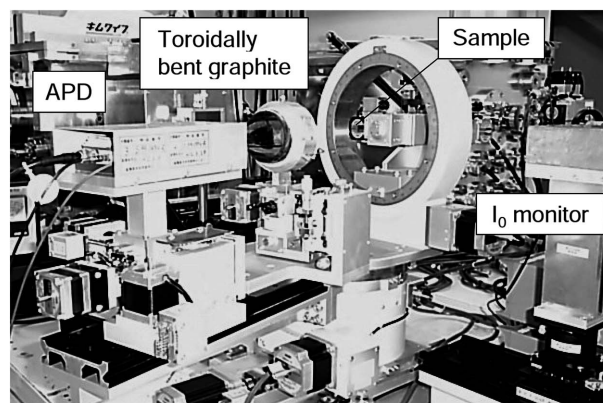
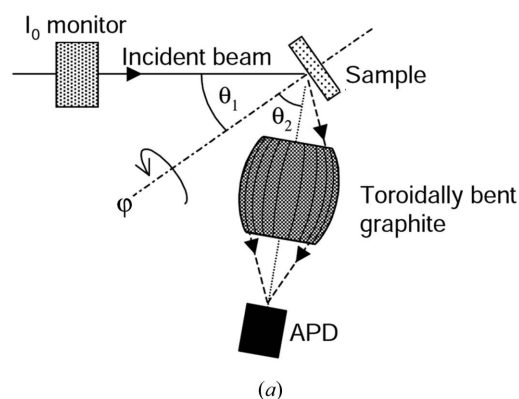


Figure 1 Schematic illustration (a) and photograph (b) of the experimental set-up.

symmetrically equivalent data were summed up, referring to these XSW lines.

The XSW lines in the hologram pattern for the irradiated sample are less clear than those for the unirradiated sample. This can be attributed to the deterioration of the crystalline structure in the irradiated sample caused by the heavy-ion bombardment. Since there was no obvious difference in the peak widths of the XRD spectra for unirradiated and irradiated samples, this implies that serious deterioration was not found in the crystalline structure along the *c*-axis caused by the heavy-ion bombardment. On the other hand, more serious deterioration was found in the in-plane crystalline structure by the heavy-ion bombardment. Fig. 3 shows reconstructed atomic images in the plane perpendicular to the *c*-axis of the unirradiated (*a*) and irradiated (*b*) EBCO specimens on the same intensity scale. The emitter (Cu) is at the center of the figure. The nearest and the second-nearest Cu atomic positions around the emitter (Cu) are shown by dashed circles. These images are constructed by utilizing the five holograms for 18.0, 18.25, 18.5, 18.75 and 19.0 keV photon energies using the Barton algorithm (Barton, 1988). The images of the nearest Cu atoms around the emitter (Cu) are obtained both in the unirradiated and irradiated specimens. We can also see atom-like images in the positions of the second-nearest atoms both in the unirradiated and irradiated specimens. However,

since these images are as weak as the artifact images and their positions are shifted from the actual positions, we cannot recognize these images as true atomic images. As we can see, the intensity of the images of the nearest Cu atoms in the irradiated specimen is weaker and broader than that of the unirradiated specimen.

Figs. 4(*a*) and 4(*b*) show the one-dimensional distribution of the real part of the reconstructed atomic images near the atomic position of the emitter (Cu), (*a*) in the radial direction relative to the emitter (Cu), *i.e.* the horizontal direction in Fig. 3, and (*b*) in the direction perpendicular to that, *i.e.* the vertical direction in Fig. 3, for the unirradiated (solid line) and irradiated specimen (dotted line). The Barton multiple-energy reconstruction algorithm gives the atomic images as negative peaks in the real parts of the reconstructions. In Fig. 4, the real-part values were inverted to avoid confusion.

For high-energy heavy-ion irradiations, production of a cylindrical damaged region along the ion beam path can be expected. The volume fraction of the damaged region, δ , is given by

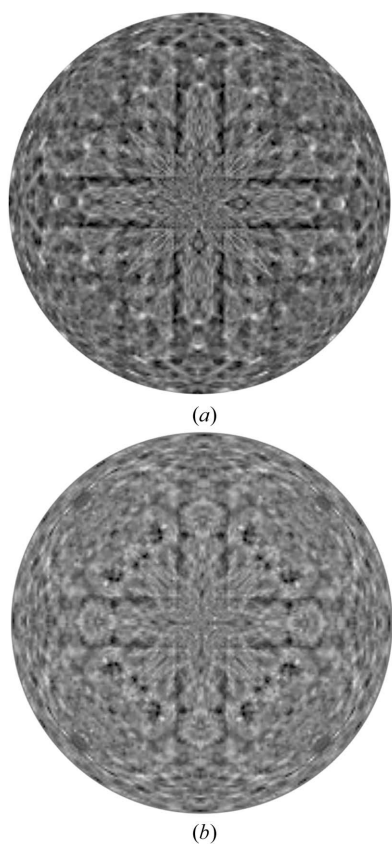


Figure 2
Holograms of unirradiated (*a*) and irradiated (*b*) EBCO with 210 MeV I ions at a fluence of $5 \times 10^{11} \text{ cm}^{-2}$, measured at a photon energy of 18.0 keV.

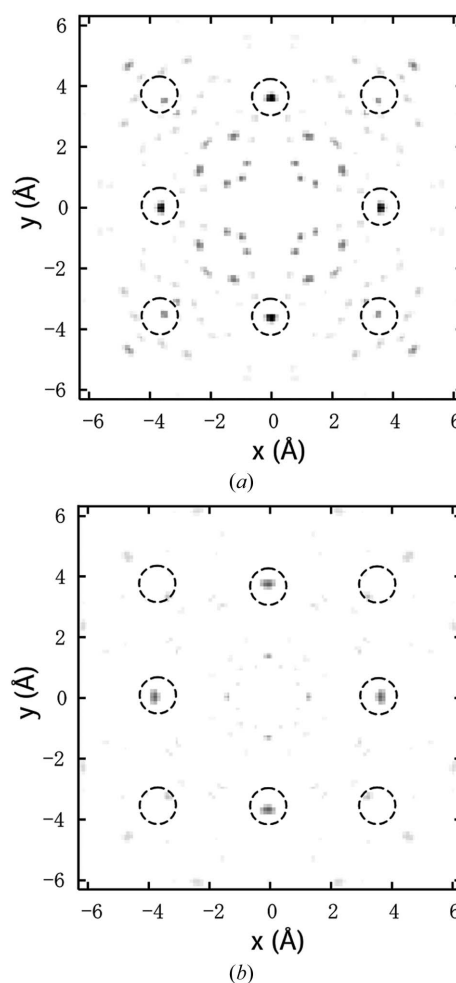


Figure 3
Reconstructed atomic images in the plane perpendicular to the *c*-axis of unirradiated (*a*) and irradiated (*b*) EBCO specimens, on the same intensity scale. The emitter (Cu) is at the center of each figure. The nearest and the second-nearest Cu atomic positions around the emitter (Cu) are shown by dashed circles.

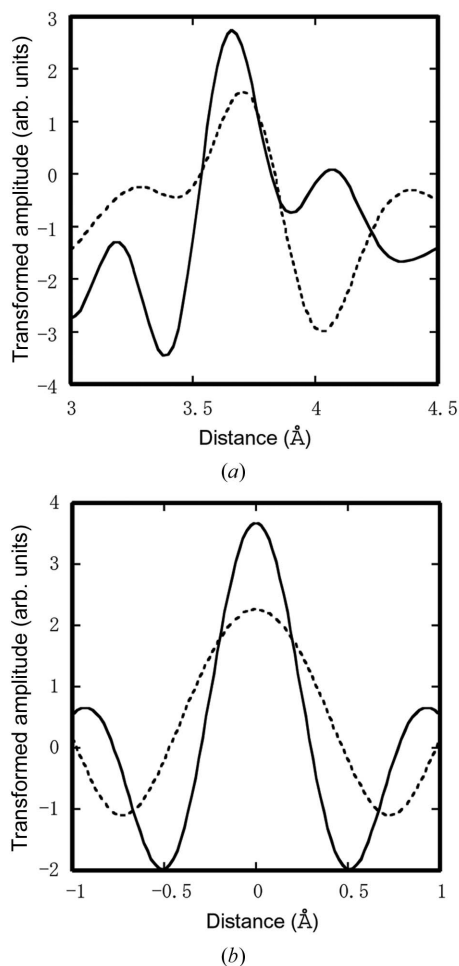


Figure 4
One-dimensional distribution of the real part of the reconstructed atomic images near the atomic position of the emitter (Cu), (a) in the radial direction relative to the emitter (Cu), *i.e.* the horizontal direction in Fig. 3, and (b) in the direction perpendicular to that, *i.e.* the vertical direction in Fig. 3, for the unirradiated (solid line) and irradiated (dotted line) specimen.

$$\delta = 1 - \exp(-A\Phi), \quad (1)$$

where $A = \pi D^2/4$ is the cross section of the damaged region and D is its diameter, and Φ is the ion fluence. From the dependence of the electrical resistivity on the ion fluence, the values of D are 10 ± 2 nm for all irradiation (Zhu *et al.*, 1993). According to (1), the volume fraction of the damaged region is estimated to be 35% at a fluence of 5×10^{11} cm⁻². The damaged region is thought to have been expanded compared with that in the crystalline state, causing a relative increase of the *c*-axis lattice parameter in the non-damaged region owing to the stress. These facts suggest that the in-plane crystalline structure change, *e.g.* lattice distortion, has also occurred owing to the stress, and the reason for the peak broadening in

the irradiated sample is the slight change in the positions of the neighboring Cu atom caused by the lattice distortion.

4. Summary

We installed a new toroidally bent graphite analyzer in the XFH system and measured holograms of EBCO thin films. Remarkable differences between unirradiated and irradiated specimens were observed in the holograms and the reconstructed atomic images. Broadening of atomic images of the irradiated sample implies the occurrence of the distortion of the Cu sub-lattice owing to the production of a cylindrical damaged region along the ion beam path.

The synchrotron radiation experiments were performed at SPring-8 with the approval of the Japan Synchrotron Radiation Research Institute (JASRI) (Proposal No. 2003A0115-NS2-np). The XRD measurements and the MEXH data analyses were performed under the Inter-University Cooperative Research Program of the Institute for Materials Research, Tohoku University. This work was financially supported in part by the Industrial Technology Research Grant Program in 2000 from the New Energy and Industrial Development Organization (NEDO) of Japan, and by a Grant-in-Aid for Scientific Research from the Japanese Ministry of Education, Culture, Sports, Science and Technology.

References

- Barton, J. J. (1988). *Phys. Rev. Lett.* **61**, 1356–1359.
 Blatter, G., Feigel'man, M. V., Geshkenbein, V. B., Larkin, A. I. & Vinokur, V. M. (1994). *Rev. Mod. Phys.* **66**, 1125–1388.
 Gog, T., Len, P. M., Materlik, G., Bahr, D., Fadley, C. S. & Sanchez-Hanke, C. (1996). *Phys. Rev. Lett.* **76**, 3132–3135.
 Harp, G. R., Saldin, D. K. & Tonner, B. P. (1990). *Phys. Rev. Lett.* **65**, 1012–1015.
 Hayashi, K., Matsui, M., Awakura, Y., Kaneyoshi, T., Tanida, H. & Ishii, M. (2001). *Phys. Rev. B*, **63**, R041201.1–R041201.4.
 Hayashi, K., Miyake, M., Tobioka, T., Awakura, Y., Suzuki, M. & Hayakawa, S. (2001). *Nucl. Instrum. Methods A*, **467/468**, 1241–1244.
 Hayashi, K., Takahashi, Y., Yonenaga, I. & Matsubara, E. (2004). *Mater. Trans.* **45**, 1994–1997.
 Iwase, A., Ishikawa, N., Chimi, Y., Tsuru, K., Wakana, H., Michikami, O. & Kambara, T. (1998). *Nucl. Instrum. Methods B*, **146**, 557–564.
 Marchesini, S., Schmithüsen, F., Tegze, M., Faigel, G., Calvayrac, Y., Belakhovsky, M., Chevrier, J. & Simionovici, A. S. (2000). *Phys. Rev. Lett.* **85**, 4723–4726.
 Michikami, O., Asahi, M. & Asano, H. (1990). *Jpn. J. Appl. Phys.* **29**, L298–L301.
 Szöke, A. (1986). *AIP Conf. Proc.* **147**, 361.
 Takahashi, Y., Hayashi, K., Matsubara, E., Shima, T., Takahashi, K., Mori, T. & Tanaka, M. (2003). *Scr. Mater.* **48**, 975–979.
 Tegze, M. & Faigel, G. (1996). *Nature (London)*, **380**, 49–51.
 Zhu, Y., Cai, Z. X., Budhani, R. C., Suenaga, M. & Welchi, D. O. (1993). *Phys. Rev. B*, **48**, 6436–6450.